RAPID COMMUNICATIONS

PHYSICAL REVIEW E VOLUME 48, NUMBER 6 DECEMBER 1993

Coexistence of morphologies in diffusive patterning

Ofer Shochet and Eshel Ben-Jacob

School of Physics and Astronomy, Raymond and Beverly Sackler Faculty of Exact Sciences, Tel Aviv University, Tel Aviv 69978, Israel

and Institute for Theoretical Physics, University of California, Santa Barbara, California 93106

(Received 7 July 1993)

We discuss a proposed morphology-selection principle and the implied concepts of the morphology diagram and morphology transitions. We use a diffusion transition scheme to demonstrate that morphology transitions can be characterized by a change in the functional form of the growth velocities and a change in the the envelope shapes. Our main support of the present picture is the demonstration of the coexistence of two morphologies, tip splitting and dendritic growth.

PACS number(s): 64.60.−i, 05.70.Ln, 64.70.Dv, 02.70.Rw

I. INTRODUCTION

With the discovery of the "microscopic solvability" criterion [1,2], the problem of dendritic growth was widely believed to be solved [3,4]. There was already an understanding of the basic mechanisms controlling either dendritic growth or tip-splitting growth. Yet, this was far from being the full picture. According to the solvability criteria, as long as anisotropy is present, needle-crystal solutions exist for any value of undercooling. However, in numerical simulations and in experiments it was found that, as the undercooling is changed at some critical value, the emerging pattern is no longer dendritic. Instead, tip splitting occurs [5–9]. The observation of the dense-branching morphology (DBM) under growth conditions, for which we know (according to the solvability criteria) that dendritic growth can exist, means that the two morphologies theoretically coexist. Thus, the microscopic solvability can clearly be only part of the picture, and a more general principle is needed to distinguish between different morphologies and to determine the one to be selected [10].

Motivated by experimental observations of pattern determination in the Hele-Shaw cell, Ben-Jacob *et al.* have proposed the existence of a morphology-selection principle [11]: in the presence of anisotropy, both tip-splitting and dendritic solutions exist, but the fastest growing morphology is the dynamically selected one. In general, if more than one morphology is a possible solution, only the "fastest growing morphology" is nonlinearly stable and will be observed.

The existence of a morphology-selection principle implies the existence of a morphology diagram, in analogy with phase diagrams in equilibrium. It further implies the existence of morphology transitions; that is, a sharp transition between morphologies occurs with a varying of the growth conditions. Similarly, observations of a sharp transition between morphologies would imply the existence of a morphology-selection principle.

Clearly different shapes are observed for the same system as we vary the control parameter (e.g., undercooling, supersaturation, etc.). However, observation of different shapes is necessary but by no means a sufficient condition to imply the existence of a morphology diagram. The simpler possibility is that the change in shape is merely a crossover and not a transition. That is, for each value of the driving force a unique solution (shape) exists. This being the case, the observed shapes can still be organized on the space of the controlled parameters (e.g., concentration and applied voltage for electrochemical deposition, anisotropy, and applied pressure for the Hele-Shaw cell, etc.). Moreover, various shapes can be classified and the parameter space can be divided into rough regimes according to the classification. However, in this case the boundaries between these regimes are fuzzy and there are no sharp transitions as the boundaries are crossed (by varying the growth parameters). Theoretically, the most important point is that for this case there is no need for the existence of a morphology-selection principle.

At present, morphology diagrams have been constructed for various experimental systems [5–9,12,13]. Unfortunately these findings are not sufficient to prove the existence of a selection principle, as the observed boundaries are quite fuzzy (presumably because of a high noise level). It is practically impossible to distinguish between a sharp crossover and a smeared (due to noise) transition. As a step to resolve this problem it was proposed to use the growth velocity as a response function and to correlate changes in the velocity with changes in the shape. Indeed, both changes in the slope of the velocity (as function of the driving force) and even jumps in its value were observed upon crossing the boundaries between morphologies [10–14]. Recently, Brener *et al.* [15] studied morphology diagrams and morphology transitions using scaling arguments and Ihle and Müller-Krumbhaar [16] studied these issues in the context of the free boundary model.

The theoretical framework presented above is still met with considerable scepticism. The main argument is that tip splitting is not a "real" solution but is observed merely because the system has a high level of noise. Hence, for some range of the parameters while the needle-crystal solution (obtained from the microscopic solvability) is linearly stable, it breaks into a tip-splitting growth due to nonlinear instability. According to this view, there is no morphology transition, but simply a crossover

from dendrites to tip splitting when noise dominates the growth.

Naturally, the best demonstration of the morphology-selection principle would be to show the existence of both morphologies for regimes where we usually observe only one of them. As we know theoretically that dendritic growth exists for regimes where DBM is observed, we specifically would like to demonstrate the existence of DBM where usually dendrites are observed. The purpose of this paper is to do exactly that.

II. ENVELOPE DYNAMICS

Recently, we have studied morphology transitions using the diffusion-transition model inspired by solidification from a supersaturated solution [17]. It is a hybridization of the "atomistic" and the continuous approaches. The dynamics of the model consists of two alternating stages: (1) Solving the linear diffusion equation for the concentration field. (2) Performing discrete phase-transition processes at the interface. We divide the phase-transition process into local processes of the solidification and melting of single cells. Only liquid cells adjacent to the solid can solidify and only solid perimeter cells can melt. The processes of phase transition and diffusion are executed sequentially on a square lattice. For more details see Ref. [17].

Both tip splitting and dendritic growth can be observed as we vary the level of supersaturation. In Figs. 1(a) and 1(b) we show two such realizations of late-stage growth. Looking at the two shapes, we can easily distinguish one from the other. The task becomes harder for shapes grown close to the transition point, which is actually the interesting regime to study. A second look will reveal that we can draw an envelope around each of the shapes (one of the equal concentration curves close to the solid can be used). Doing so, it becomes clear that the shapes of the DBM and the dendritic envelopes are different: convex for the first and concave for the second. This observation suggests the use of the envelope as our tool for the geometrical characterization of the morphologies. For both morphologies the envelope is shape preserving and propagates at constant velocity, as demonstrated in Figs. 1(c) and 1(d). Here the envelope is ensemble averaged. Thirty different realizations were grown for each set of growth conditions and the envelope was defined to be the 0.5 contour curve of the projection of all realizations. (Keep in mind that the solid concentration in the model is defined to be 1.) Clearly, such a definition of the envelope is not practical for experimental observations. Alternatively, since we know that the envelope is shape preserving and advances at constant velocity, we can also construct the envelope for a single growth realization by projection of the scaled (by the radius) shapes at different time steps, as is demonstrated in Fig. 2. The time-scaled envelope is much rougher than the ensemble-averaged envelope since Kardar-Parisi-Zhang (KPZ)–like fluctuations do not decay [18]. In order to reveal the smooth envelope for the single realization, one may use the fact that the growing pattern's symmetry reflects the lattice anisotropy. Therefore, in our case, we can average over the fourfold symmetry and reveal a smooth envelope similar to the ensemble-averaged one.

In Fig. 3 we show how the average envelope changes as a function of the driving force (the chemical potential difference), from concave for dendrites to convex for DBM. The shape of the envelope also describes the angle dependence of the velocity, $v(\theta)$ (θ is the angle). Regarding the shape as an equilibrium shape, we can perform the inverse Wulff construction to calculate an effective dynamical interfacial energy as a function of θ. For dendrites, the concave regimes at 45° of the main growth directions correspond to a multivalued effective interfacial energy. It can be understood as follows: the 45° regimes can be filled equally by sidebranches emitted from main trunks on either sides. Hence, if we consider the dynamical interfacial energy for the envelope as a function describing the the dynamics of sidebranches, it should be multivalued at 45°. In other words, a concave envelope goes hand in hand with underlying orientation of the sidebranches

FIGURES

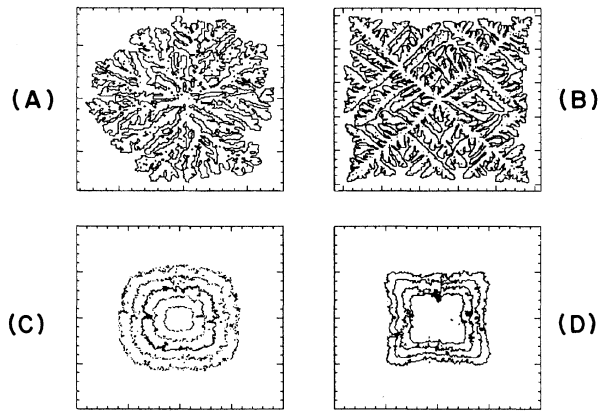

FIG. 1. (a) Typical realization of dense-branching growth. (b) Typical realization of dendritic growth. (c) Time sequence of an ensemble-averaged envelope of dense-branching growth over 30 different realizations. The envelope is shape preserving, convex, and shows a pronounced fourfold symmetry. (d) Time sequence of an ensemble-averaged envelope of dendritic growth. In this case, the envelope is concave.

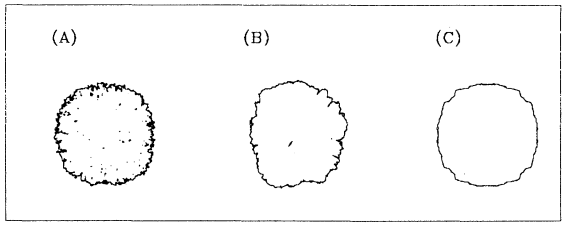

FIG. 2. (a) Ensemble-averaged envelope. (b) Time scaled averaged envelope of single realization. It has much higher fluctuations and demonstrates the long "lifetime"of the initial deformations. (c) Time scaled averaged envelope for a single realization with averaging over the lattice symmetry. By this method one may reveal a smooth envelope using just one realization.

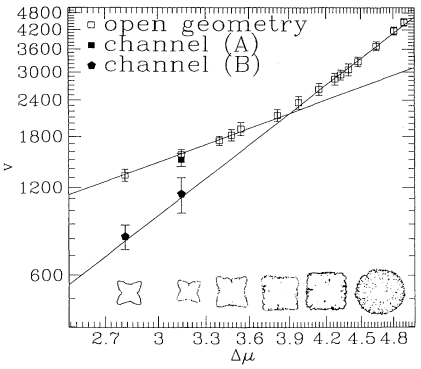

FIG. 3. The envelope shapes and growth velocity v as function of the driving force $\Delta\mu$ (log-log plot). The envelope shapes drawn at the bottom are ensemble averaged over 30 different realizations and change from concave (for dendrites) to convex (for DBM). Least-squares-fit changes from 1.5 for dendrites to 3.0 for DBM. $\omega = 8000$, $-\mu_s/T = 2.83 - 5.26$, $E_B/T = 2.66$, $D = 10^4$, $c_\infty = 0.7$, and the system size is 400×400.

and can be used to distinguish between DBM and dendritic growth. The switching of the effective interfacial energy from being multivalued to single-valued at the transition point provides additional support to the idea of morphology transitions.

III. VELOCITY AS A RESPONSE FUNCTION

It was proposed that, as the average velocity measures the rate of approach towards equilibrium, it might serve as a response function [10,11]. By the term "average velocity" one should refer to the velocity weighted according to the geometry of the interface, and thus take into account the global shape of the object. The motivation was as follows: For solidification from the supersaturated solution the entropy production (per unit length) at the interface (denoted here by Γ) is proportional to $v\Delta\mu_i$, where $\Delta\mu_i$ is the chemical potential difference between the solid chemical potential and the liquid chemical potential at the interface.

A fundamental question is whether Γ is the only variable; i.e., whether Γ plays a role analogous to the free energy of systems in equilibrium, or whether there are two parts, one of them Γ and the other, let us name it Ω, is a measure of the microscopic and mesoscopic level organization (i.e., Ω is a measure of the static properties). In this view, Γ is analogous to the entropy and Ω (which is yet to be defined) is the analogue of the internal energy.

In Fig. 3 we show the functional dependence of the DBM and dendrite's maximal velocities on the driving force $\Delta\mu$. Here $\Delta\mu$ is the difference between the solid chemical potential and the liquid chemical potential at infinity. Each point on the graph indicates the averaged velocity (in the 45° direction) over 30 realizations. The error bars indicate the standard deviation of the measurements. Although the range of $\Delta\mu$ is too small for accurate measurements of the exponent, clearly the velocity has a different functional dependence for the two morphologies. It appears to scale as

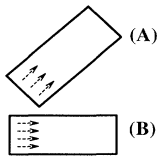

FIG. 4. The channels used for simulations. (a) Channel along the 45° orientation of the lattice. (b) Channel along the 0° orientation of the lattice.

$$v \propto \begin{cases} (\Delta\mu)^3 & \text{DBM} \\ (\Delta\mu)^{1.5} & \text{dendrites.} \end{cases} \quad (1)$$

The different scaling of the velocity indicates that indeed the velocity, hence Γ, is a suitable candidate to serve as a response function. Moreover, the two lines (Fig. 3) cross exactly at the transition point from the concave to the convex envelope ($\Delta\mu_c \simeq 4$).

IV. MORPHOLOGY COEXISTENCE

The next step in the study of morphology selection is to demonstrate morphology coexistence. To this end we have simulated the growth in a channel geometry. Two different channels were used: (a) A channel along the preferred direction for dendritic growth [45° off the lattice directions—Fig. 4(a)]. (b) A channel along the lattice direction [Fig. 4(b)]. The growth velocities for these channels are presented in Fig. 3. In simulations of growth in the first channel (a) the growth velocity follows that of the open geometry for all ranges of parameters. For $\Delta\mu < \Delta\mu_c$ dendritic morphology is observed and the growth velocity is the same as the growth velocity for the open geometry (i.e., $v \propto \Delta\mu^{1.5}$). For higher $\Delta\mu$, DBM is observed and the growth velocity is, again, the same as for the open geometry (i.e., $v \propto \Delta\mu^{3.0}$).

The simulation of growth in the second channel

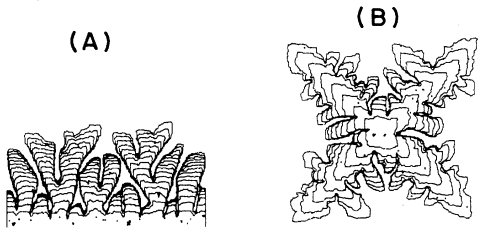

FIG. 5. The effect of the growth geometry on the morphology. The two stroboscopic pictures also show the difference in growth velocity between both morphologies, as the time elapsed between two consecutive snapshots is the same in both plots. ($\omega = 8000$, $-\mu_s/T = 2.8$, $E_B/T = 2.66$, $D = 10^4$, $c_\infty = 0.7$, and the system size is 400×400.) (a) Tip-splitting growth is observed in a channel. (b) Dendritic growth is observed for the same parameter in a channel. The total simulation steps are half of those for (a), as the velocity is much higher.

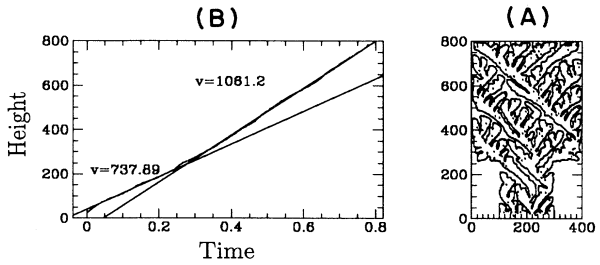

FIG. 6. Growth starting from a narrow channel and spreading into a wider channel. (a) DBM growth is observed in the narrow part while dendritic growth with pronounced 45° orientation is observed in the wider part. (b) The maximum height of the pattern vs time. For the narrow channel the growth velocity is slower and fits the $v \propto \Delta\mu^{3.0}$ line. In the wider channel, the growth velocity is faster and fits the $v \propto \Delta\mu^{1.5}$ line.

[Fig. 4(b)] leads to the expected result: DBM is observed for all range of parameters as the dendritic growth is suppressed by the geometrical constraints (see Fig. 5). Furthermore, the growth velocity for all values of $\Delta\mu$ follows the scaling of the DBM growth ($v \propto \Delta\mu^3$). This is our demonstration of the coexistence of the two morphologies.

We further connected a narrow channel with a wider one. Growth patterns for parameters of the original dendritic regime are presented in Fig. 6(a). The simulation was started from an initial seed at the narrow part of the channel. At the beginning, inside the narrow channel, tip-splitting growth occurs. The growth velocity [Fig. 6(b)] for the narrow part fits the $v \propto \Delta\mu^{3.0}$ line of the open-geometry DBM regime. At the widening point of the channel, there is less competition between the fingers, and dendritic growth at 45° is observed. The growth velocity at this stage switches to fit the $v \propto \Delta\mu^{1.5}$ of the dendritic regime. In the wider channel, as some of the fingers are more advanced into the liquid than the other ones, dendritic morphologies may continue in a zig-zag-like growth. As the growth simulation is based on a stochastic process, we have also observed (usually in wide channels) spontaneous transitions between dendritic growth and tip-splitting growth. In some rare cases, the growth in the narrow channel may be dendritic due to a spatial fluctuation in which one of the fingers shoots out and emits sidebranches. These rare simulation results are included in the standard deviation calculation for the channel simulations in Fig. 3.

To conclude, our observations provide a strong support for the coexistence of DBM and dendritic growth. Hence, the "microscopic solvability" can clearly be merely a part of the picture, and a more general selection principle is needed to select one of the morphologies. The "fastest growing" selection principle seems to hold for many cases. Yet, further studies are required to identify its range of applicability.

ACKNOWLEDGMENTS

The diffusion-transition scheme was developed in collaboration with K. Kassner, S. G. Lipson, and H. Müller-Krumbhaar [17]. We thank M. Azbel, H. Levine, L. Kadanoff, and R. Kupferman for useful discussions. We thank the Institute for Theoretical Physics and the participants of the program in "Spatially Extended Nonequilibrium Systems" for hospitality and discussions. This research was supported in part by a grant from the GIF, the German-Israeli Foundation for Scientific Research and Development, by NSF Grant No. PHY89-04035, and by the Program for Alternative Thinking at Tel-Aviv University.

[1] E. Ben-Jacob, N. Goldenfeld, B. G. Kotliar, and J. S. Langer, Phys. Rev. Lett. **53**, 2110 (1984).
[2] D. A. Kessler, J. Koplik, and H. Levine, Phys. Rev. A **31**, 1712 (1985).
[3] D. A. Kessler, J. Koplik, and H. Levine, Adv. Phys. **37**, 255 (1988).
[4] J. S. Langer, Science **243**, 1150 (1989).
[5] E. Ben-Jacob, R. Godbey, N. D. Goldenfeld, J. Koplik, H. Levine, T. Mueller, and L. M. Sander, Phys. Rev. Lett. **55**, 1315 (1985).
[6] V. Horvath, T. Vicsek, and J. Kertesz, Phys. Rev. A **35**, 2353 (1987).
[7] A. Buka and P. Palffy-Muhoray, Phys. Rev. A **36**, 1527 (1987).
[8] P. Oswald, J. Bechhoefer, and F. Melo, Mater. Res. Bull. **16**, 38 (1991).
[9] Rong-Fu Xiao *et al.* Phys. Rev. E **47**, 3463 (1993).
[10] E. Ben-Jacob and P. Garik, Nature **343**, 523 (1990).
[11] E. Ben-Jacob, P Garik, T. Muller, and D. Grier, Phys. Rev. A **38**, 1370 (1988).
[12] Y. Sawada, A. Dougherty, and J. P. Gollub, Phys. Rev. Lett. **56**, 1260 (1986).
[13] D. G. Grier, E. Ben-Jacob, R. Clarke, and L. M. Sander, Phys. Rev. Lett. **56**, 1264 (1986).
[14] S. K. Chan, H. H. Reimer, and M. Kahlweit, J. Cryst. Growth **32**, 303 (1976).
[15] E. A. Brener, H. Müller-Krumbhaar, and D. E. Temkin, Europhys. Lett. **17**, 535 (1992).
[16] T. Ihle and H. Müller-Krumbhaar, Phys. Rev. Lett. **70**, 3083 (1993).
[17] O. Shochet, K. Kassner, E. Ben-Jacob, S. G. Lipson, and H. M. Müller-Krumbhaar, Physica A **181**, 136 (1992); **197**, 87 (1992).
[18] M. Kardar, G. Parisi, and Y. C. Zhang, Phys. Rev. Lett. **56**, 889 (1986).